On the electronic structure of the hydrogenase H-cluster†‡

David E. Schwab,[a] Cedric Tard,[b] Eric Brecht,[a] John W. Peters,[a] Christopher J. Pickett[bc] and Robert K. Szilagyi*[a]

Received (in Berkeley, CA, USA) 7th April 2006, Accepted 28th June 2006
First published as an Advance Article on the web 31st July 2006
DOI: 10.1039/b604994j

X-ray absorption spectroscopic measurements and density functional calculations suggest that the hydrogenase H-cluster is best described as an electronically inseparable 6Fe-cluster due to extensive delocalization of frontier molecular orbitals of the iron centres, sulfide and the non-innocent dithiolate ligands.

The active site of FeFe-hydrogenases has attracted considerable attention due to its unusual organometallic nature and potential implications in the design of dihydrogen production/uptake systems. Crystallographic studies of the FeFe-hydrogenases from two microorganisms (*Cp*[1] and *Dd*[2]) converged to a common structure for the active site.[3] Thus 'classical' [4Fe–4S] and organometallic [2Fe–2S] units are connected by a bridging cysteine to form the catalytic assembly, the H-cluster (Fig. 1A). The coordination environment of the 2Fe-subcluster is completed with water, carbonyl and cyanide ligands, and a bridging dithiolate ligand. Crystallographic,[3] Mössbauer,[4,5] EPR,[6] ENDOR,[7] and FTIR[8] spectroscopic results suggest a diamagnetic [$4Fe^{(2.5+)}$–4S] and an $S = 1/2$ [$Fe^{(I)}Fe^{(II)}$–2S] subcluster with bridging CO and terminal CN^-/CO ligands for the resting form of the protein bound H-cluster. Change of iron oxidation states during catalysis, the CO/CN^- ligand arrangement, and the dithiolate composition are yet to be confirmed by direct experiments.

Earlier computational investigations primarily focused on the 2Fe-subcluster[10–13] as the catalytically active centre. Recent studies considered the linked 4Fe- and 2Fe-subclusters of the first biomimetic cluster assembly[9] and the metalloenzyme's complete active site.[14,15] The most recent theoretical study[15] provided insights into the role of the 4Fe-subcluster by exploring the geometric and magnetic properties of the entire 6Fe-cluster. However, the electronic structure, and the *g*- and *A*-values were only evaluated for a truncated model without including the 4Fe-subcluster. These calculations qualitatively reproduced the trends in EPR parameters, gave good agreement with the exchange parameters, and emphasized the structural importance of 4Fe-subcluster in determining the bridging S(Cys)–Fe distances. In this communication, we report the first direct experimental evidences for an electronic role of the bridging dithiolate, and demonstrate the coupling between the subclusters using X-ray absorption spectroscopy[16] and density functional theory.[17] Details of the measurements and computations are summarized in the ESI.†

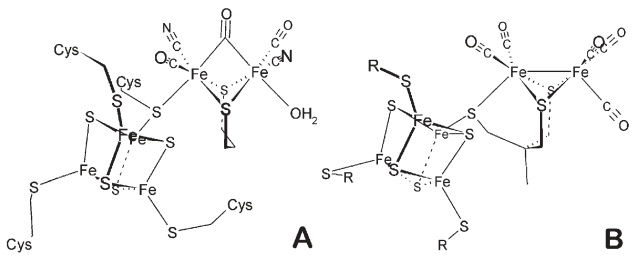

Fig. 1 Schematic structures of the hydrogenase H-cluster[1] (A) and the H-cluster framework[9] (B).

The distinct structure of the 2Fe-subcluster, relative to 'classical' [2Fe–2S] clusters,[18] implies unique roles for the dithiolate ligand of the H-cluster. So far, catalytic importance has been suggested for the dithiomethylammine (dtma) ligand,[19–21] as the amino group in the β-position can provide a convenient site for proton transfer. Sulfur K-edge XAS measurements for a series of structurally well-defined complexes ([$Fe_2^{(I)}(LS_2)(CO)_6$]) suggest that the composition of the ligand also affects the redox active orbitals of the 2Fe-subcluster. This emerging technique[16] probes the sulfur 3p-based, antibonding metal-ligand orbitals. Thus, it provides a direct experimental handle to quantify the bonding interactions from spectral features below the ionization threshold (edge jump). The energy positions of the pre- and rising-edge features are informative of the sulfur charge and the metal d-manifold energy; the intensities reflect the covalence of the metal–sulfur bonds.

On the basis of intense pre-edge features between 2471 and 2473 eV (Fig. 2), the studied binuclear model compounds can be described with covalent Fe–S bonds. In going from sulfide (black), to thiolate (blue), and to dithiolate (red and green spectra), the changes in pre-edge intensities are consistent with gradually diminishing Fe–S bond covalence. The constrained distance between the sulfurs in propanadithiolate (pdt) increases the ligand–ligand repulsion and reduces the Fe–S overlap, relative to the free thiolates, giving rise to a less covalent bonding. The weakened Fe–S bonding parallels with shorter Fe…Fe distances (Fig. 2). The reduced electron donation from sulfurs, the increased Fe–Fe bonding, and the shift of the pre-edge features to lower energy are indicative of more electrophilic metal centres for complexes with dithiolate ligands relative to sulfide ligands. Furthermore, the greater electronegativity of the secondary amine in dtma relative to the β-methylene group in pdt reduces the nucleophilicity of the thiolate sulfurs and thus further weakens the Fe–S bonds. These spectral differences suggest that the chemical

[a]*Department of Chemistry and Biochemistry, Montana State University, Bozeman, MT59718, USA. E-mail: Szilagyi@Montana.EDU*
[b]*Department of Chemical Biology, John Innes Research Centre, Norwich, UK NR4 7TJ*
[c]*School of Chemical Sciences and Pharmacy, University of East Anglia, Norwich, UK NR4 7TJ*

† Electronic supplementary information (ESI) available: Details of experimental setup, data analysis, and computational methods; Cartesian coordinates of computational models; frontier orbital contour plots. See DOI: 10.1039/b604994j

‡ RKS dedicates this paper to the 70th birthday of Professor Lajos Bencze, University of Veszprém, Hungary.

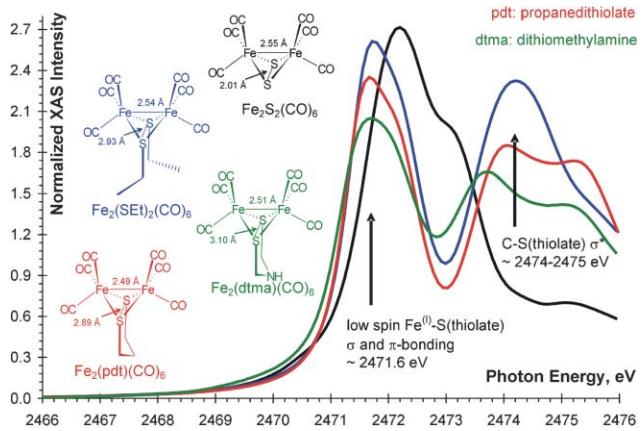

Fig. 2 Sulfur K-edge spectra of inorganic model complexes for the 2Fe-subcluster with different sulfur ligand bridges.

composition of the dithiolate ligand has a significant affect on the electronic structure of the 2Fe-subcluster *via* perturbation of the Fe–S bond.

The recent synthesis of the H-cluster framework[9] (Fig. 1B) allowed for direct measurements of the electronic coupling between the subclusters. Carbonyl stretching frequencies, reduction potentials, and photoelectron spectroscopic results[9] have already indicated the delocalization of electron density between the two subclusters. While the coordination environment and the oxidation state of the iron centres in the 2Fe-subcluster of the framework are somewhat different from those of the protein bound H-cluster, the bridging thiolate link between the two subclusters, which is the focus of this study, is present in both structures. Differences in sulfur K-edge XAS spectra in Fig. 3 (green solid and dotted lines) directly demonstrate the extensive delocalization of the inorganic sulfide character from the 4Fe-subcluster into the 2Fe subcluster. The green and the blue spectra in Fig. 3 correspond to the model complex with H-cluster framework and a [4Fe–4S] cluster, respectively, with identical terminal thiolate ligands. The difference of their spectra renormalized for three sulfur absorbers (black line), as done for the [2Fe–3S] model in Fig. 3 (brown line), shows two

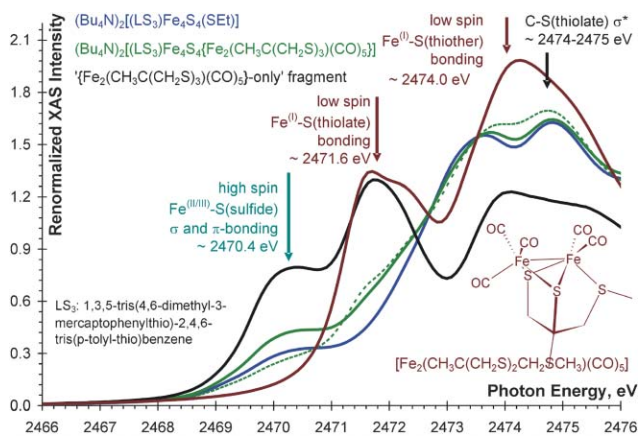

Fig. 3 Renormalized difference sulfur K-edge spectrum (black line) between the 6Fe-cluster (green solid line measured, dotted line predicted spectrum without delocalization) and 4Fe-cluster (blue lines) and comparison to a relevant 2Fe-cluster (brown line).

pre-edge features with maxima at 2470.4 and 2471.6 eV. The latter is observed in the spectra of 2Fe-subcluster models in Figs. 2 and 3 and indicative of low spin $Fe^{(I)}$–S bonding. The former can be assigned to the Fe–S(sulfide) and Fe–S(thiolate) transition envelope in 4Fe models[16] that are absent in the 2Fe models. Therefore, its presence is indicative of sulfide character in unoccupied orbitals that are delocalized between the two subclusters.

Density functional calculations using BP86 functionals and effective core potentials with triple-ζ quality valence basis set (see ESI for more detail†) on the entire 6Fe model (115 atoms) with identical coordination environment to the experimentally measured compound $([(LS_3)Fe_4S_4\{Fe_2(CH_3C(\mu\text{-}SCH_2)_3(CO)_5)\}]^{2-}$ with $[Fe(^{2.5+})_4S_4]^{2+}$ $\{Fe^{(I)}{}_2S_2\}^0$ subclusters in S_t = 0 spin state) further support the electronic coupling between the two subclusters. This level of theory has been validated using experimental geometric and electronic structural data.[17] The optimized structure of the H-cluster framework is close to the available experimental structures[22,23] with slightly longer Fe–S bond lengths (Fig. 4) than obtained by De Gioga.[9] The difference contour plot between the electron densities of the entire 6Fe model and the sum of the separate 4Fe- and 2Fe-subclusters in the 6Fe model geometry (Fig. 4) illustrates the extent of electronic structural changes upon formation of the (μ-SCH_2)–Fe(4Fe) bond between $[(LS_3)Fe_4S_4]^{1-}$ and $[Fe_2(CH_3C(\mu\text{-}SCH_2)_3)(CO)_5]^{1-}$ subclusters. The atomic spin densities of the 2Fe-subcluster with low-spin $Fe^{(I)}$ ions are smaller relative to the 4Fe-subcluster (Fig. 4) due to electron delocalization of both spin up (α) and spin down (β) orbitals of the 2Fe-subcluster. The shape of the most dominant lobes in Fig. 4 clearly suggests that the delocalization involves the Fe $3d_{z^2}$ orbitals from the 2Fe-subcluster in addition to thiolate C–S σ and CO π orbitals. Frontier molecular orbitals in Fig. S1 provides more detail about the anatomy of the electron delocalization.†

Due to the inherent limitation§ of the data analysis of the structurally characterized, native FeFe-hydrogenases from *Cp*[1] and *Dd*[2] we use the calibrated density functional theory to connect our observations for the biomimetic framework with the protein bound H-cluster. These calculations on a computational model $([(EtS)_3Fe_4S_4(\mu\text{-}SEt)Fe_2(pdt)(\mu\text{-}CO)(CN)_2(CO)_2(OH_2)]^{3-}$, with $[Fe(^{2.5+})_4S_4]^{2+}$ $\{Fe^{(I/II)}{}_2S_2\}^{1+}$ subclusters in S_t = 1/2 spin state) of the composite structure of the H-cluster in its resting form provide very similar electron density differences (Fig. S3)† and frontier

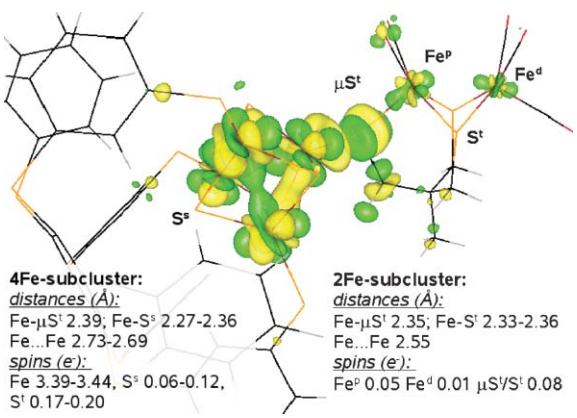

Fig. 4 Electron density difference plot (yellow/green are ±0.003 contours) between the 6Fe-cluster and separate 4Fe- and 2Fe-subclusters.

orbital plots (Fig. S4)† to the H-cluster framework and thus suggest the delocalization of molecular orbitals between the two subclusters independently from the oxidation state and CO/CN ligand environment of the 2Fe subcluster. It is interesting to note that for the active site model, the HOMO-s have greater contributions from the 2Fe-subcluster, which can facilitate the oxidative addition of dihydrogen, while the dominant 4Fe-subcluster character in the LUMO-s can aide the electron transfer into the H-cluster for proton reduction.

In the light of the presented spectroscopic and computational results we conclude that the hydrogenase H-cluster is an electronically inseparable 6Fe-cluster due to the significant delocalization of molecular orbitals. Perturbations to this electronic coupling are expected to play a key role in determining the dihydrogen binding or protonation and the reversibility of the redox chemistry at the hydrogenase active site.

Portions of this research were carried out at the Stanford Synchrotron Radiation Laboratory (proposal number 2893), a national user facility operated by Stanford University on behalf of the U.S. Department of Energy, Office of Basic Energy Sciences. The SSRL Structural Molecular Biology Program is supported by the Department of Energy, Office of Biological and Environmental Research, and by the National Institutes of Health, National Centre for Research Resources, Biomedical Technology Program RKS acknowledges funding from NSF EPSCoR, ONR CBIN, and NIH INBRE. CJP and CT thank the BBSRC and the John Innes Foundation for support. JWP acknowledges financial support from NSF and AFOSR.

Notes and references

§ We have collected XAS data for native and CO-inhibited forms of the FeFe-hydrogenase *Cp*I (Fig. S2)†; however, due to overlapping spectral features of the accessory iron–sulfur clusters of the enzyme and the background of numerous methionine sulfurs the data cannot be used for quantitative analysis. Recent results[24] concerning the successful heterologous expression of FeFe-hydrogenases in *E. coli* provide a viable approach to reduce the background.

1 J. W. Peters, W. N. Lanzilotta, B. J. Lemon and L. C. Seefeldt, *Science*, 1998, **282**, 1853–1858.
2 Y. Nicolet, C. Piras, P. Legrand, C. E. Hatchikian and J. C. Fontecilla-Camps, *Struct. Fold Des.*, 1999, **7**, 13–23.
3 Y. Nicolet, B. J. Lemon, J. C. Fontecilla-Camps and J. W. Peters, *Trends Biochem. Sci.*, 2000, **25**, 138–143.
4 C. V. Popescu and E. Münck, *J. Am. Chem. Soc.*, 1999, **121**, 7877–7884.
5 A. S. Pereira, P. Tavares, I. Moura, J. J. G. Moura and B. H. Huynh, *J. Am. Chem. Soc.*, 2001, **123**, 2771–2782.
6 K. K. Surerus, M. Chen, J. W. Vanderzwaan, F. M. Rusnak, M. Kolk, E. C. Duin, S. P. J. Albracht and E. Munck, *Biochemistry*, 1994, **33**, 4980–4993.
7 J. Telser, M. J. Benetsky, M. W. W. Adams, L. E. Mortenson and B. M. Hoffman, *J. Biol. Chem.*, 1987, **262**, 6589–6594.
8 A. L. De Lacey, C. Stadler, C. Cavazza, E. C. Hatchikian and V. M. Fernandez, *J. Am. Chem. Soc.*, 2000, **122**, 11232–11233.
9 C. Tard, X. M. Liu, S. K. Ibrahim, M. Bruschi, L. De Gioia, S. C. Davies, X. Yang, L. S. Wang, G. Sawers and C. J. Pickett, *Nature*, 2005, **433**, 610–613.
10 Z. X. Cao and M. B. Hall, *J. Am. Chem. Soc.*, 2001, **123**, 3734–3742.
11 Z. P. Liu and P. Hu, *J. Am. Chem. Soc.*, 2002, **124**, 5175–5182.
12 M. Bruschi, P. Fantucci and L. De Gioia, *Inorg. Chem.*, 2002, **41**, 1421–1429.
13 I. P. Georgakaki, L. M. Thomson, E. J. Lyon, M. B. Hall and M. Y. Darensbourg, *Coord. Chem. Rev.*, 2003, **238–239**, 255–266.
14 T. Zhou, Y. Mo, Z. Zhou and K. Tsai, *Inorg. Chem.*, 2005, **44**, 4941–4946.
15 A. Friedler and T. C. Brunold, *Inorg. Chem.*, 2005, **44**, 9322–9334.
16 E. I. Solomon, B. Hedman, K. O. Hodgson, A. Dey and R. K. Szilagyi, *Coord. Chem. Rev.*, 2005, **249**, 97–129.
17 R. K. Szilagyi and M. A. Winslow, *J. Comput. Chem.*, 2006, **27**, 1385–1397.
18 P. Venkateswarea Rao and R. H. Holm, *Chem. Rev.*, 2004, **104**, 527–559.
19 Y. Nicolet, A. L. de Lacey, X. Vernede, V. M. Fernandez, E. C. Hatchikian and J. C. Fontecilla-Camps, *J. Am. Chem. Soc.*, 2001, **123**, 1596–1601.
20 H.-J. Fan and M. B. Hall, *J. Am. Chem. Soc.*, 2001, **123**, 3828–3829.
21 R. M. Henry, D. L. Shoemaker, D. L. DuBois and M. Rakowski DuBois, *J. Am. Chem. Soc.*, 2006, **128**, 3002–3010.
22 P. V. Rao, S. Bhaduri, J. Jiang, D. Hong and R. H. Holm, *J. Am. Chem. Soc.*, 2005, **127**, 1933–1945.
23 M. Razavet, S. C. Davies, D. L. Hughes, J. E. Barclay, D. J. Evans, S. A. Fairhurst, X. Liu and C. J. Pickett, *Dalton Trans.*, 2003, 586–585.
24 M. C. Posewitz, P. W. King, S. L. Smolinski, R. D. Smith, A. R. Ginley, M. L. Ghirardi and M. Seibert, *Biochem. Soc. Trans.*, 2005, **33**, 102–104.

